Published in final edited form as:
*Cancer Res*. 2011 February 1; 71(3): 964–975. doi:10.1158/0008-5472.CAN-10-3172.

# Disruption of a *Sirt1* Dependent Autophagy Checkpoint in the Prostate Results in Prostatic Intraepithelial Neoplasia Lesion Formation

**Michael J. Powell**[1], **Mathew C. Casimiro**[1], **Carlos Cordon-Cardo**[2], **Xiaohong He**[3], **Wen-Shuz Yeow**[1], **Chenguang Wang**[1], **Peter A. McCue**[1], **Michael W. McBurney**[3], and **Richard G. Pestell**[1,*]

[1]Departments of Cancer Biology and Oncology, Kimmel Cancer Center, Thomas Jefferson University, Philadelphia, Pennsylvania, 19107, USA

[2]Department of Pathology and Urology, Herbert Irving Comprehensive Cancer Center, Columbia University, New York, New York, 10032, USA

[3]Departments of Medicine and Biochemistry, Microbiology and Immunology, Ottawa Health Research Institute, University of Ottawa, Ottawa, Canada K1H8L6

## Abstract

The Sirtuin family of proteins (SIRTs) encode a group of evolutionarily conserved, NAD-dependent histone deacetylases, involved in many biological pathways. SIRT1, the human homolog of the yeast Silent Information Regulator 2 (*Sir2*) gene, deacetylates histones, p300, p53, and the androgen receptor. Autophagy is required for the degradation of damaged organelles and long-lived proteins, as well as for the development of glands such as the breast and prostate. Herein, homozygous deletion of the *Sirt1* gene in mice resulted in prostatic intraepithelial neoplasia (PIN) associated with reduced autophagy. Genome-wide gene expression analysis of *Sirt1*$^{-/-}$ prostates demonstrated that endogenous *Sirt1* repressed androgen responsive gene expression and induced autophagy in the prostate. *Sirt1* induction of autophagy occurred at the level of autophagosome maturation and completion in cultured prostate cancer cells. These studies provide novel evidence for a checkpoint function of *Sirt1* in the development of prostatic intraepithelial neoplasia and further highlight a role for SIRT1 as a tumor suppressor in the prostate.

### Keywords

SIRT1; Prostatic Intraepithelial Neoplasia (PIN); Prostate; Autophagy; Tumor Suppressor

## Introduction

The sirtuin family consists of NAD$^+$-dependent histone deacetylases (HDACs), conserved from *archaeobacteria* to *eukaryotes*, and classified as class III HDACs (1,2). The enzymatic activity of sirtuins is NAD$^+$ dependent and the Sirtuin family members (SIRT1-SIRT7), convey diverse functions (2). SIRT1 is the mammalian ortholog of the *Sir2* gene, an

*Corresponding Author: Richard G. Pestell, Kimmel Cancer Center, Department of Cancer Biology, Thomas Jefferson University, 233 South 10th Street, Philadelphia, PA 19107, Tel: 213-503-5692; Fax: 215-503-9334.
For Reprints: cecilia.deemer@kimmelcancercenter.org

The authors declare no conflict of interest as they pertain to this manuscript.

important regulator of aging in *Saccharomyces Cerevisiae*, *Caenorhabditis Elegans*, and *Drosophila Melanogaster* (3). The role of SIRT1 in cellular growth control is complex and cell-type specific. *In vitro*, SIRT1 inhibits p53, Bax, Ku70, FOXO, and the retinoblastoma (Rb) protein (4,5), which may be anticipated to promote cell proliferation. Reduction in SIRT1 activity induced cell growth arrest and apoptosis in breast, lung, and colon cancer cells (5-7). Inhibition of SIRT1 with Sirtinol induced growth arrest in MCF7 and H1299 cells (5). In contrast, several *in vivo* studies suggest that SIRT1 may function as a tumor suppressor as *Sirt1*$^{-/-}$ mice show an impaired DNA damage response, evident by increased genomic instability and tumorigenesis (8). Additional studies from *Sirt1*$^{-/-}$ and transgenic mice are consistent with a role for *Sirt1* in tumor suppression as *Sirt1* was shown to suppress intestinal tumorigenesis and colon cancer (9).

Androgen receptor (AR) expression and activity are key determinants of prostate cancer onset and progression. Of potential importance to prostate biology and function, SIRT1 deacetylates the histone acetyltransferase (HAT) p300 and the AR. SIRT1 transduction of AR-expressing prostate cancer cells (LNCaP) decreased cell proliferation and blocked contact-independent growth (10). The AR colocalizes with SIRT1 in a nuclear sub-compartment, where SIRT1 binds to and deacetylates the AR, thereby inhibiting its activity (1,11). Histone acetyltransferases (p300, CBP/PCAF, Tip60) acetylate the AR at a conserved motif in response to dihydroxytestosterone (DHT), thereby stimulating the growth and anti-apoptotic functions of the AR. The AR lysine residues targeted by acetylation (K630, K632, K633) are well conserved between species and serve as substrates for SIRT1-mediated deacetylation (12,13), resulting in inhibition of ligand-induced AR activity (14).

Prostate cancer proceeds via morphological changes transitioning from the development of prostatic intraepithelial neoplasia (PIN), invasive adenocarcinoma, and metastasis. The pathognomonic features of PIN include changes in nuclear morphology such as enlargement of the nucleus and nucleolus. Molecular genetic dissection in the mouse demonstrated that forced expression of c-Myc (15), Akt, or deletion of Pten (16) leads to PIN and/or prostate adenocarcinoma.

The role of SIRT1 in regulating prostate gland formation and androgen signaling *in vivo* was previously unknown. SIRT1 is expressed in several cell types in the prostate gland including basal cells, luminal cells, and stromal cells. Given the evidence that SIRT1 functions as a tissue-specific regulator of cellular growth and that SIRT1 inhibits tumor cell line growth in nude mice, we sought to determine the role of endogenous *Sirt1* in regulating prostate gland development. Genome-wide expression profiling of *Sirt1*$^{-/-}$ mice prostates and their littermate controls identified a molecular, genetic signature regulated by endogenous *Sirt1*. This signature highlights the ability of *Sirt1* to inhibit androgen signaling and apoptosis in the prostate, while promoting autophagy. The *Sirt1*$^{-/-}$ prostates demonstrated epithelial hyperplasia and prostatic intraepithelial neoplasia (PIN) suggesting that *Sirt1* promotes autophagy and inhibits prostate epithelial cell proliferation *in vivo*.

## Materials and Methods

### Gross Anatomical Analysis

*Sirt1*$^{-/-}$ mice and littermate controls aged 2-3 months were euthanized by $CO_2$ asphyxiation and subsequently weighed and measured for both mass and length. Animals were dissected with the following organs being removed: ventrodorsolateral prostate, anterior prostate, seminal vesicles, testes, epididymus, vas deferens, kidneys, liver, spleen, and pancreas. Portions of each organ were fixed in 4% paraformaldehyde to be used for sectioning and Hematoxylin and Eosin (H&E) staining. Ki67 staining was performed as previously described (17).

### Transgenic Mice and Genotyping

All *Sirt1* transgenic mice used were provided by Dr. Michael McBurney and have been previously described (18). The appropriate institutional committee approved protocols were employed when working with these mice. RT-PCR analysis to confirm the genotype of the mice used was conducted through genotyping with oligonucleotides directed toward exon 5 of *Sirt1*, generating a 132 bp amplimer (nucleotide sequences were forward: 5′ AATATATCCCGGACAGTTCCAGCC 3′ and reverse: 5′ ATCCTTTGGATTCCTGCAACCTGC 3′).

### Microarray and Pathway Analysis

5μg of total RNA derived from *Sirt1*$^{+/+}$ and *Sirt1*$^{-/-}$ ventrodorsolateral prostates (Trizol Reagent, Invitrogen, Carlsbad, CA) was reverse transcribed using Superscript III First-Strand Synthesis System (Invitrogen) using an HPLC purified T7-dT24 primer (Sigma Genosys, St. Louis, MO) containing the T7 polymerase promoter sequence. Single stranded cDNA was converted to double stranded cDNA using DNA polymerase I (Promega, Madison, WI) and purified by cDNA spin column purification using a GeneChip Sample Cleanup Module (Affymetrix, Santa Clara, CA). Double stranded cDNA was used as a template to generate biotinylated cDNA using Bioarray HighYield RNA Transcription Labeling Kit (Enzo, New York, NY). cRNA (15μg) was fractionated to produce fragments of between 35-200 bp using 5× fragmentation buffer provided in the Cleanup Module. Samples were hybridized to a mouse 430A 2.0 microarray (Affymetrix) representing approximately 14,000 well-characterized genes. Hybridization and washing steps were carried out in accordance with Affymetrix protocols for eukaryotic arrays. Arrays were scanned at 570nm with an Affymetrix confocal scanner.

Analysis of arrays was performed using the R statistics package (19) and the limma library (20) of the Bioconductor software package. Arrays were normalized using robust multiarray analysis (RMA), while a P-value of 0.05 and a fold change of at least 2 fold was applied as criteria for statistically differentially expressed genes. Gene Ontology (GO) analysis of gene functions was analyzed using “Webgestalt” (http://bioinfo.vanderbilt.edu/webgestalt). Genes were clustered using hierarchical clustering with “complete” agglomeration. Each cluster was further analyzed based on the known function of the genes contained in the cluster. Expression profiles are displayed using Treeview (21). Pathway analysis was performed using the following databases: Kyoto Encyclopedia of Genes and Genomes (KEGG), BioCarta, Gene Set Enrichment Analysis (GSEA), Analysis of Sample Set Enrichment Scores (ASSESS) and the Database for Annotation, Visualization and Integrated Discovery (DAVID).

### LC3 Immunofluorescence

LNCaP cells (American Type Culture Collection, Manassas, VA) transfected with either pcDNA3 or pcDNA3-SIRT1 (Lipofectin, Invitrogen, Carlsbad, CA) were plated on Poly-L-Lysine (Sigma, St. Louis, MO)-coated chamber slides (Nunc, Rochester, NY) in either complete media (CM: RPMI, 10% FBS, 1% Penicillin-Streptomycin, 1% L-Glutamine) or serum free media (SFM: RPMI, 1% Penicillin-Streptomycin, 1% L-Glutamine). After 24hrs, half of the cells plated with SFM were treated with 10nM DHT (SFMA) for 24hrs. All other cells were treated with vehicle (ethanol) control. After DHT treatment, media was removed and cells were washed twice with PBS. Next, cells were fixed with 4% paraformaldehyde (Electron Microscopy Sciences, Hatfield, PA) for 15min at room temperature, followed by a 5min PBS wash and a 10min 1× PBS + 0.1% Triton wash. Cells were then incubated at room temperature for 1hr in 1% PBS-BSA+0.05% Triton. Afterward, cells were incubated at 4°C overnight with gentle shaking in primary antibody (LC3-II, Abgent, San Diego, CA, 1:50) prepared in PBS+0.05% Triton. Next, cells were washed with PBS-BSA three times,

followed by treatment with secondary antibody in PBS+0.05% Triton (Alexa-Fluor 488 goat anti-rabbit, Invitrogen, 1:1000) for 1hr at room temperature. Cells were then washed with PBS three times, mounted (Prolong Gold antifade reagent with DAPI, Invitrogen), coverslipped, and examined by confocal microscopy (Zeiss LSM 510 META Confocal Microscope System, Germany).

### Western Blot and siRNA Knockdown

Western blotting was performed as previously described (10) using 50μg of whole cell lysates prepared following cell treatments. Antibodies used included anti-LC3 (Novus, Littleton, CO, 1:500), anti-SIRT1 (Santa Cruz: H-300, Santa Cruz, CA, 1:1000), anti-GAPDH (Santa Cruz: FL-335, 1:1000), anti-ATG4c (Abcam: ab-75056, Cambridge, MA, 1:500), anti-Beclin1 (Santa Cruz: H-300, 1:500), anti-AR (Millipore: PG-21, Billerica, MA, 1:1000), and anti-GDIα (22). Knockdown experiments were performed as previously described (23), (24). siRNAs used included SIRT1 siRNA (Qiagen: SI00098434, Valencia, CA) and a validated, non-silencing control siRNA (Qiagen: 10227281). Quantitation and normalization of immunoblotting results was performed as previously described (25).

## Results

### Sirt1$^{-/-}$ Mice Develop Prostatic Intraepithelial Neoplasia

To examine the role of *Sirt1* in the development of androgen-responsive tissues such as the prostate, *Sirt1*$^{-/-}$ mice were examined. Genotyping was conducted as previously described (18) and analysis of *Sirt1* mRNA abundance conducted by RT-PCR of prostate tissue confirmed no detectable *Sirt1* mRNA in *Sirt1*$^{-/-}$ prostates (Fig. 1A). Morphological analysis of *Sirt1*$^{+/+}$and *Sirt1*$^{-/-}$ mice showed that average body length and weight were decreased in the *Sirt1*$^{-/-}$ mice (Fig. 1B,C). Individual organ weights were measured and normalized to the animal's body weight (Fig. 1D). The ventrodorsolateral (VDL) and anterior prostates and the seminal vesicles were significantly decreased in size when normalized to total body weight (Fig. 1D). In contrast, the weight of the intestine and pancreas was unchanged (Fig. S1A). The epididymal fat pad was increased in size, with a modest, but significant reduction in the normalized weight of the liver and kidney in the *Sirt1*$^{-/-}$ mice (Fig. S1A). Collectively, these studies demonstrate that endogenous *Sirt1* plays a role in the development of androgen-responsive tissues.

Histological analysis of the *Sirt1*$^{-/-}$ mice tissues was conducted (Fig. 1E,S1B). Prostates were smaller in *Sirt1*$^{-/-}$ mice compared to *Sirt1*$^{+/+}$ littermate controls with a larger stromal layer (Fig. 1D,E). The *Sirt1*$^{-/-}$ prostates exhibited a morphological phenotype similar to that commonly observed within prostatic intraepithelial neoplasia (PIN) lesions, accompanied by increased cellularity and nuclear atypia (Fig. 1E), a phenotype confirmed to remain without further disease progression in 7 month old *Sirt1*$^{-/-}$ mice (data not shown). *Sirt1*$^{-/-}$ prostates showed glandular hyperplasia and an increased Ki67 proliferative index (Fig.1E,F). The epididymis of the *Sirt1*$^{-/-}$ mice was hypoplastic, while the seminal vesicles were smaller in size and demonstrated a large stromal layer surrounding the epithelium (Fig. S1B). The seminiferous tubules were dilated with a significant reduction in the number of mature sperm within the *Sirt1*$^{-/-}$ mice (Fig. S1B).

### Sirt1 Governs Prostate Autophagy, Apoptosis, and Cell Proliferation Signaling Pathways

To examine the gene expression profile regulated by endogenous *Sirt1*, ventrodorsolateral prostate RNA from *Sirt1*$^{+/+}$ and *Sirt1*$^{-/-}$ mice was compared. 498 genes were differentially regulated by *Sirt1*, with 146 mRNAs altered greater than two-fold (Fig. 2A). The biological pathways associated with this altered gene expression signature analyzed using Biocarta and the Kyoto Encyclopedia of Genes and Genomes (KEGG) demonstrated that endogenous

*Sirt1* regulates pathways governing the cell cycle, cell adhesion, diabetes, and immune function (Tables S1,S2). Comparisons made with published datasets of androgen-responsive genes identified in prostate cancer cell lines or within the prostate gland (Tables S4A,B), displayed an overlap between *Sirt1*-regulated and androgen-regulated genes as 12.45% of the genes regulated by *Sirt1* were also previously reported to be androgen-responsive. Several genes induced by DHT *in vitro* correspond to genes repressed by *Sirt1* in the prostate and similarly *Sirt1* enhanced expression of several genes repressed by DHT. For other genes, directionality of expression changes by DHT and *Sirt1* were concordant (Tables S3-S4B). The highest proportion of genes coinciding with our data was found with *in vivo* data (22/498, 4.42%) rather than cultured prostate cancer cell lines (26). This finding suggests that androgen signaling may differ between the *in vivo* and cultured cell environment.

Higher order structural analysis of the expression data was conducted using gene set enrichment analysis (GSEA) and Analysis of Sample Set Enrichment Scores (ASSESS) to identify discrete biological functions associated with cell signaling in our array. GSEA utilizes gene expression levels as a means to establish a set rank list of significantly regulated genes within compared sample populations. ASSESS refers to a measure of enrichment of the gene sets across multiple established and annotated gene sets (27). Supervised clustering was employed and identified a set of biological pathways in which the expression profiles were altered upon deletion of *Sirt1*. Such pathways included cell motility, chemotaxis, cell adhesion, and cell cycle (Fig. 2B,S1C). Additional pathway and enrichment analysis was performed using the Database for Annotation, Visualization and Integrated Discovery (DAVID) database. These analyses confirmed similar biological pathways governed by endogenous *Sirt1* in the prostate including autophagy, apoptosis, and cell proliferation (Fig. 2C). *Sirt1* regulated the expression of *Atg4*, *Atg7*, and *Atg8* in the prostate. These genes are required for late-stage autophagy including phagophore elongation, maturation, and autophagosome vesicle formation (Fig. 2C). This biological role for *Sirt1* in the promotion of autophagy was further confirmed by ASSESS pathway analysis, as a defined set of genes up-regulated following rapamycin treatment and mTOR (mechanistic target of rapamycin) inhibition (known autophagic stimulants) were also promoted by *Sirt1* in the prostate (Fig. S1C).

## SIRT1 Inhibits AR-Dependent Repression of Autophagy

In view of our finding that *Sirt1* induced gene expression pathways associated with autophagy, we conducted tissue culture-based experiments to determine the effects of SIRT1 on autophagy in prostate cancer cells. Formation of autophagosomes can be assayed by the sub-cellular distribution of LC3 (microtubule-associated protein 1 light chain 3 alpha), the mammalian homologue of the *Atg8* gene. A hallmark of mammalian autophagy is the conversion of LC3-I to LC3-II via proteolytic cleavage and lipidation. This modification of LC3 is essential for the formation of autophagosomes and for the completion of macroautophagy. Additionally, the LC3-GFP fusion protein can be used as a surrogate measure of autophagy through the formation of “LC3 punctae or dots” (28).

To validate our microarray results, AR-expressing prostate cancer cells (LNCaP) were treated with either control siRNA or siRNA directed against SIRT1. Whole cell lysates were subjected to immunoblotting for SIRT1 and autophagy markers, ATG4c, LC3-I, and LC3-II. Following SIRT1 knockdown, the abundance of these proteins decreased suggesting that SIRT1 promotes autophagy in prostate cancer cells (Fig. 3A). Western blots performed using protein isolated from the ventrodorsolateral prostates of $Sirt1^{+/+}$ and $Sirt1^{-/-}$ mice further confirmed a decrease in the abundance of autophagy markers (*Atg4c, Atg6 (Beclin1), and Atg8 (LC3)*) and an increase in AR abundance in the $Sirt1^{-/-}$ prostate (Fig. S3A). Next, LNCaP cells were transfected with either an expression vector encoding SIRT1 or a control

vector (pcDNA3). After transfection, cells were cultured in the presence (CM) or absence of serum (SFM, autophagy stimulant) and treated with either vehicle or DHT and subjected to immunofluorescence (IF) for either LC3-II (Fig. 3B-D) or IgG control (Fig. S2A). Our results indicated that serum deprivation induced autophagy when compared with complete media (Fig. 3B,C) and that 10nM DHT (SFMA) inhibited serum withdrawal-induced autophagy (Fig. 3C,D). Furthermore, transfection of cells with SIRT1 enhanced autophagy and abrogated DHT-mediated inhibition of autophagy (Fig. 3B-D). Cells were counted and graded based on abundance of LC3-II positive staining. The number of LC3-II positive cells and severity of autophagic response per cell (defined according to number of autophagosomes present per cell) was increased following SIRT1 transfection, regardless of serum or androgen presence (Fig. 3E,F). SIRT1 Western blot analysis following transfection confirms that the levels of SIRT1 post-transfection fall within physiological levels as previously described (29). Cells were also co-transfected with GFP to confirm transfection efficiency (>80% GFP positive cells post-transfection) (Fig. 3G).

Immunoblotting confirmed the induction of LC3-II by serum deprivation. SIRT1 transfection of LNCaP cells further enhanced the formation of LC3-II in both complete growth media and in serum-deprived media (Fig. 4A). SIRT1 induced the abundance of the autophagy-related proteins ATG5, ATG6 (Beclin1) and ATG9 (Data Not Shown). The SIRT1 antagonist Sirtinol enhanced DHT-mediated repression of autophagy (Fig. 4B). Collectively, these studies demonstrate that SIRT1 antagonizes DHT-mediated repression of autophagy, an effect that can be abolished by Sirtinol-mediated SIRT1 inhibition.

The formation of acidic, vesicular organelles (AVOs) in the cell cytoplasm, which can be stained by acridine orange (AO) (22), is an additional measure of autophagy. Punctate, cytoplasmic staining in the CY3 wavelength is indicative of autophagolysosome formation and autophagy. Fluorescence in the FITC channel is indicative of AO staining of DNA, while accumulation of red staining in the nucleolus of cells represents AO staining of RNA. Acridine orange staining demonstrated the presence of AVOs in the absence of serum and in the presence of SIRT1, the formation of which was inhibited by both Sirtinol and/or physiological concentrations of DHT (Figs. S2B,C,S3B,C).

An additional surrogate measure of AVO formation and active autophagy is staining with monodansylcadaverine (MDC) (30). Transfection of LNCaP cells with SIRT1 resulted in an increase in the intensity and abundance of MDC positive staining regardless of serum or androgen presence compared to pcDNA3 vector control, consistent with our prior results. Conversely, similar effects were blocked by treatment with the SIRT1 inhibitor, Sirtinol (Fig. S4A-C).

To examine further the mechanism by which SIRT1 regulates autophagy in prostate cancer cells, LNCaP cells were transduced with either MSCV-IRES-GFP or MSCV-IRES-SIRT1-GFP retroviruses and subsequently sorted by GFP expression (Fig. 4C). Cells were GFP sorted and stained with MDC or AO and analyzed by confocal microscopy. Cells transduced with SIRT1 exhibited heightened AVO formation in both the presence and absence of autophagic stimuli (serum) and androgens (Figs. S4D-F,S5,S6). Co-immunofluorescence for LC3, SIRT1 (Fig. 4D,E), GFP, and IgG controls (Figs. S7A-D) was also performed on these cells in the presence and absence of autophagic stimuli (Hank's Balanced Buffer Solution, HBSS, Gibco/Invitrogen). HBSS was shown to increase the autophagic response as evident by an increase in LC3 positive staining (Fig. 4D,E). This effect appears to be mediated at some level through SIRT1 as HBSS treatment stimulated SIRT1 expression in MSCV-IRES-GFP transduced cells (Fig. 4D). The abundance of LC3 staining and severity of the autophagic response was enhanced in MSCV-IRES-SIRT1-GFP transduced cells (Fig. 4E). Notably, HBSS treatment of these cells stimulated a shift of SIRT1 expression from a

primarily nuclear distribution to a more uniform distribution throughout the nucleus and cytosol. This observation could be explained by the ability of HBSS to induce cellular stress, in turn triggering SIRT1 to transfer into the cytosol where it may deacetylate and activate late-stage autophagy related genes to finalize the induction of autophagy and protect the cell from stress.

LNCaP cells stably expressing either GFP (LNCaP-GFP) or the LC3-GFP fusion protein (LNCaP-LC3-GFP) were established. These cells were sequentially transfected with either pcDNA3 or SIRT1, treated with either vehicle or DHT, and analyzed by confocal microscopy for the appearance of GFP-positive, LC3 punctae (Fig. 5A-D). SIRT1 induced the formation of LC3 punctae, which was reversed upon inhibition of SIRT1 with Sirtinol (Figs. 5A-D,6A,B).

Herein we demonstrate that endogenous *Sirt1* inhibits murine prostate epithelial cell proliferation. *Sirt1*$^{-/-}$ prostates demonstrate increased Ki67 staining, prostatic hyperplasia, and prostatic intraepithelial neoplasia. *Sirt1* promoted autophagy in the prostate, functioning at the level of autophagosome maturation and vesicle formation (Fig. 7).

## Discussion

Cancer is characterized by a series of transitions from normal to preneoplastic, invasive, and metastatic disease. The checkpoints to progression of early phenotypic transitions in this process are increasingly well understood. Cellular senescence, the angiogenic switch, and epithelial-mesenchymal transitions may represent barriers to transitions throughout the tumorigenic phenotype. The current studies identify a role for endogenous *Sirt1* as a key regulator of normal prostate gland homeostasis *in vivo*, in part through its ability to modulate autophagic signaling pathways. These studies also highlight the repercussion of *Sirt1* loss in the prostate gland, as deletion of *Sirt1* results in the development of prostatic intraepithelial neoplasia (PIN). Herein, *Sirt1*$^{-/-}$ prostates were reduced in size with features of PIN. The features of PIN observed in the *Sirt1*$^{-/-}$ mice included cellular hyperplasia, increased Ki67 staining, hyperchromatic nuclei, and prominent nucleoli. These observations and the reduced size of the prostate are consistent with a role for *Sirt1* in the regulation of organ development. Previously defined regulators of murine PIN (activation of the Akt pathway, c-myc, or p27$^{KIP1}$) were not observed in the *Sirt1*$^{-/-}$ prostate, suggesting *Sirt1* regulates PIN via an alternative mechanism. Genome-wide microarray and pathway analysis demonstrated that endogenous *Sirt1* regulates pathways governing apoptosis, cell proliferation, Ras signaling, androgen signaling and autophagy in the prostate. The finding that *Sirt1* inhibits Ras signaling is consistent with recent studies in which SIRT1 inhibited growth of Ras-transformed cells in nude mice (31) and inhibited LNCaP cell proliferation and colony formation (10). Endogenous *Sirt1* repressed genes that promote cellular proliferation and cell cycle progression including cdc25, cyclin D2, cyclin D3, and cyclin B2. In addition, *Sirt1* repressed several growth factors and pro-proliferative cytokines including CXCL9 and CCL5.

Gene expression analysis further demonstrated that loss of endogenous *Sirt1* inhibited autophagy. At a higher level of resolution, our studies demonstrated that SIRT1 antagonized DHT-mediated inhibition of autophagy in the prostate. Autophagy allows for degradation of proteins and organelles (32,33) and is induced by nutrient withdrawal, rapamycin (inhibition of mTOR signaling), and hormone signaling (PPARγ, ERα/Tamoxifen) (22). Our findings are consistent with prior studies demonstrating that SIRT1 induces autophagy by deacetylating ATG5, 7, and 8 (34) and inhibits AR signaling via deacetylation of the AR (10). Comparisons with previously published studies identified an overlap of 12.45% between genes regulated by endogenous *Sirt1* and those targeted by androgens in the

prostate gland and in prostate cancer cells. These results are consistent with prior findings that *Sirt1* inhibits ligand-dependent AR signaling and gene expression *in vitro* (10,35).

*Sirt1* deletion and the resulting inhibition of autophagy may have contributed to the reduction in prostate size as autophagy regulates normal gland development. Mutagenesis of the *Dictyostelium* ortholog of the yeast *Atg 5,6,7,8* genes results in aberrant development (36). In *Saccharomyces Cerevisiae*, autophagy is essential for differentiation and sporulation (37), and in *Caenorhabditis Elegans*, bec-1 (ATG6/VPS30/Beclin1) is essential for dauer diapause formation (38). Mice defective in autophagy have shown defective tissue development as conditional *Atg5* and *Atg7* knockout mice demonstrate neuronal and hepatic abnormalities (39,40). Autophagy has also been implicated in tissue remodeling associated with duct formation in breast and prostate cells *in vitro* and in 3D matrigel (41). Prostatic 3D cultures also form hollow, acinus-like structures that stain strongly for LC3 (42). Autophagy has pro-survival and pro-death functions (43). A pro-survival function for autophagy is evidenced by a loss of autophagy resulting in death of both *C. Elegans* and *D. Melanogaster* (37,38). In contrast, autophagy can also be pro-death. Knockdown of Atg's inhibits non-apoptotic cell death (44). These studies suggest that physiological levels of autophagy are pro-survival, whereas an excessive level of autophagy promotes autophagic cell death (45).

The role of autophagy in cancer was proposed over 20 years ago (46). Autophagy appears to be essential for tumor suppression as well as for cell survival (47). Autophagy plays a pro-survival function for cancer cells during nutrient deprivation or when apoptotic pathways are compromised, a phenotype often accompanied by inflammation. In contrast, upon disruption of tumor suppressors, autophagy adopts a pro-death role with apoptotic pathways (48). In prostate, breast, ovarian, and lung cancer, loss of *Beclin1* or inhibition of *Beclin1* by the BCL-2 family of proteins causes defective autophagy, increased DNA damage, metabolic stress, and genomic instability. These cancers also display neoplastic changes and increased cell proliferation, unlike cells over-expressing *Beclin1*, which undergo apoptosis (49,50). Loss of PTEN, p53, ATG4, ATG5, and MAP1LC31 (ATG8) are linked to tumorigenesis, while up-regulation of PI3K, AKT, BCL-2, and mTOR are associated with inhibition of autophagy and the promotion of tumorigenesis.

Prostate cancer onset and progression is correlated strongly with aging and SIRT1 function governs aging in multiple species. Further studies will be required to determine whether this checkpoint function of *Sirt1* in regards to prostate growth is linked to its role in organismal aging.

## Supplementary Material

Refer to Web version on PubMed Central for supplementary material.

## Acknowledgments

This work was supported in part by 5R01CA070896-15, 5R01CA075503-12, 2R01CA086072-07A2, 5R01CA107382-06, 1R01CA132115-01A1 (RGP). The Kimmel Cancer Center is supported by the NIH Cancer Center Core grant P30CA56036. This project is a generous grant from the Dr. Ralph and Marian C. Falk Medical Research Trust (RGP) and supported in part by a grant from the Pennsylvania Department of Health (RGP). The department disclaims responsibility for any analysis, interpretations, or conclusions. The authors declare no conflict of interest as they pertain to this manuscript.

Financial Support: 5R01CA070896-15, 5R01CA075503-12, 2R01CA086072-07A2, 5R01CA107382-06, 1R01CA132115-01A1, P30CA56036, Falk Medical Research Trust Grant, Pennsylvania Department of Health Grant

## References


1. Yang T, Fu M, Pestell R, Sauve AA. SIRT1 and endocrine signaling. Trends Endocrinol Metab 2006;17:186–91. [PubMed: 16684606]
2. Whittle JR, Powell MJ, Popov VM, Shirley LA, Wang C, Pestell RG. Sirtuins, nuclear hormone receptor acetylation and transcriptional regulation. Trends Endocrinol Metab 2007;18:356–64. [PubMed: 17964799]
3. Longo VD, Kennedy BK. Sirtuins in aging and age-related disease. Cell 2006;126:257–68. [PubMed: 16873059]
4. Lim CS. SIRT1: tumor promoter or tumor suppressor? Med Hypotheses 2006;67:341–4. [PubMed: 16546327]
5. Ota H, Tokunaga E, Chang K, Hikasa M, Iijima K, Eto M, et al. Sirt1 inhibitor, Sirtinol, induces senescence-like growth arrest with attenuated Ras-MAPK signaling in human cancer cells. Oncogene 2006;25:176–85. [PubMed: 16170353]
6. Ford J, Jiang M, Milner J. Cancer-specific functions of SIRT1 enable human epithelial cancer cell growth and survival. Cancer Res 2005;65:10457–63. [PubMed: 16288037]
7. Heltweg B, Gatbonton T, Schuler AD, Posakony J, Li H, Goehle S, et al. Antitumor activity of a small-molecule inhibitor of human silent information regulator 2 enzymes. Cancer Res 2006;66:4368–77. [PubMed: 16618762]
8. Wang RH, Sengupta K, Li C, Kim HS, Cao L, Xiao C, et al. Impaired DNA damage response, genome instability, and tumorigenesis in SIRT1 mutant mice. Cancer Cell 2008;14:312–23. [PubMed: 18835033]
9. Firestein R, Blander G, Michan S, Oberdoerffer P, Ogino S, Campbell J, et al. The SIRT1 deacetylase suppresses intestinal tumorigenesis and colon cancer growth. PLoS One 2008;3:e2020. [PubMed: 18414679]
10. Fu M, Liu M, Sauve AA, Jiao X, Zhang X, Wu X, et al. Hormonal control of androgen receptor function through SIRT1. Mol Cell Biol 2006;26:8122–35. [PubMed: 16923962]
11. Bouras T, Fu M, Sauve AA, Wang F, Quong AA, Perkins ND, et al. SIRT1 deacetylation and repression of p300 involves lysine residues 1020/1024 within the cell cycle regulatory domain 1. J Biol Chem 2005;280:10264–76. [PubMed: 15632193]
12. Fu M, Wang C, Reutens AT, Wang J, Angeletti RH, Siconolfi-Baez L, et al. p300 and p300/cAMP-response element-binding protein-associated factor acetylate the androgen receptor at sites governing hormone-dependent transactivation. J Biol Chem 2000;275:20853–60. [PubMed: 10779504]
13. Fu M, Rao M, Wang C, Sakamaki T, Wang J, Di Vizio D, et al. Acetylation of androgen receptor enhances coactivator binding and promotes prostate cancer cell growth. Mol Cell Biol 2003;23:8563–75. [PubMed: 14612401]
14. Fu M, Wang C, Wang J, Sakamaki T, Zhang X, Yeung YG, et al. The Androgen Receptor Acetylation governs transactivation and MEKK1-induced apoptosis without affecting in vitro sumoylation and transrepression function. Mol Cell Biol 2002;22:3373–88. [PubMed: 11971970]
15. Ellwood-Yen K, Graeber TG, Wongvipat J, Iruela-Arispe ML, Zhang J, Matusik R, et al. Myc-driven murine prostate cancer shares molecular features with human prostate tumors. Cancer Cell 2003;4:223–38. [PubMed: 14522256]
16. Wang S, Gao J, Lei Q, Rozengurt N, Pritchard C, Jiao J, et al. Prostate-specific deletion of the murine Pten tumor suppressor gene leads to metastatic prostate cancer. Cancer Cell 2003;4:209–21. [PubMed: 14522255]
17. Drobnjak M, Osman I, Scher HI, Fazzari M, Cordon-cardo C. Overexpression of cyclin D1 is associated with metastatic prostate cancer to bone. Clinical Cancer Research 2000;6:1891–5. [PubMed: 10815912]
18. Cheng HL, Mostoslavsky R, Saito S, Manis JP, Gu Y, Patel P, et al. Developmental defects and p53 hyperacetylation in Sir2 homolog (SIRT1)-deficient mice. Proc Natl Acad Sci U S A 2003;100:10794–9. [PubMed: 12960381]

19. Chen Y, Kamat V, Dougherty ER, Bittner ML, Meltzer PS, Trent JM. Ratio statistics of gene expression levels and applications to microarray data analysis. Bioinformatics 2002;18:1207–15. [PubMed: 12217912]
20. Smyth GK. Linear models and empirical bayes methods for assessing differential expression in microarray experiments. Stat Appl Genet Mol Biol 2004;3 Article3.
21. Eisen MB, Spellman PT, Brown PO, Botstein D. Cluster analysis and display of genome-wide expression patterns. Proc Natl Acad Sci U S A 1998;95:14863–8. [PubMed: 9843981]
22. Zhou J, Zhang W, Liang B, Casimiro MC, Whitaker-Menezes D, Wang M, et al. PPARgamma activation induces autophagy in breast cancer cells. Int J Biochem Cell Biol 2009;41:2334–42. [PubMed: 19563910]
23. Espada J, Ballestar E, Santoro R, Fraga MF, Villar-Garea A, Nemeth A, et al. Epigenetic disruption of ribosomal RNA genes and nucleolar architecture in DNA methyltransferase 1 (Dnmt1) deficient cells. Nucleic Acids Res 2007;35:2191–8. [PubMed: 17355984]
24. Chen Z, Peng IC, Cui X, Li YS, Chien S, Shyy JY. Shear stress, SIRT1, and vascular homeostasis. Proc Natl Acad Sci U S A 2010;107:10268–73. [PubMed: 20479254]
25. Miller RK, Qadota H, Stark TJ, Mercer KB, Wortham TS, Anyanful A, et al. CSN-5, a component of the COP9 signalosome complex, regulates the levels of UNC-96 and UNC-98, two components of M-lines in Caenorhabditis elegans muscle. Mol Biol Cell 2009;20:3608–16. [PubMed: 19535455]
26. Singh J, Manickam P, Shmoish M, Natik S, Denyer G, Handelsman D, et al. Annotation of androgen dependence to human prostate cancer-associated genes by microarray analysis of mouse prostate. Cancer Lett 2006;237:298–304. [PubMed: 16024171]
27. Edelman E, Porrello A, Guinney J, Balakumaran B, Bild A, Febbo PG, et al. Analysis of sample set enrichment scores: assaying the enrichment of sets of genes for individual samples in genome-wide expression profiles. Bioinformatics 2006;22:e108–16. [PubMed: 16873460]
28. Mizushima N, Yamamoto A, Matsui M, Yoshimori T, Ohsumi Y. In vivo analysis of autophagy in response to nutrient starvation using transgenic mice expressing a fluorescent autophagosome marker. Mol Biol Cell 2004;15:1101–11. [PubMed: 14699058]
29. Wei S, Kulp SK, Chen CS. Energy restriction as an antitumor target of thiazolidinediones. J Biol Chem 2010;285:9780–91. [PubMed: 20093366]
30. Li M, Jiang X, Liu D, Na Y, Gao GF, Xi Z. Autophagy protects LNCaP cells under androgen deprivation conditions. Autophagy 2008;4:54–60. [PubMed: 17993778]
31. Li Y, Xu W, McBurney MW, Longo VD. SirT1 inhibition reduces IGF-I/IRS-2/Ras/ERK1/2 signaling and protects neurons. Cell Metab 2008;8:38–48. [PubMed: 18590691]
32. Xie Z, Klionsky DJ. Autophagosome formation: core machinery and adaptations. Nat Cell Biol 2007;9:1102–9. [PubMed: 17909521]
33. Cecconi F, Levine B. The role of autophagy in mammalian development: cell makeover rather than cell death. Dev Cell 2008;15:344–57. [PubMed: 18804433]
34. Lee IH, Cao L, Mostoslavsky R, Lombard DB, Liu J, Bruns NE, et al. A role for the NAD-dependent deacetylase Sirt1 in the regulation of autophagy. Proc Natl Acad Sci U S A 2008;105:3374–9. [PubMed: 18296641]
35. Dai Y, Ngo D, Forman LW, Qin DC, Jacob J, Faller DV. Sirtuin 1 is required for antagonist-induced transcriptional repression of androgen-responsive genes by the androgen receptor. Mol Endocrinol 2007;21:1807–21. [PubMed: 17505061]
36. Otto GP, Wu MY, Kazgan N, Anderson OR, Kessin RH. Macroautophagy is required for multicellular development of the social amoeba Dictyostelium discoideum. J Biol Chem 2003;278:17636–45. [PubMed: 12626495]
37. Tsukada M, Ohsumi Y. Isolation and characterization of autophagy-defective mutants of Saccharomyces cerevisiae. FEBS Lett 1993;333:169–74. [PubMed: 8224160]
38. Melendez A, Talloczy Z, Seaman M, Eskelinen EL, Hall DH, Levine B. Autophagy genes are essential for dauer development and life-span extension in C. elegans. Science 2003;301:1387–91. [PubMed: 12958363]
39. Komatsu M, Waguri S, Chiba T, Murata S, Iwata J, Tanida I, et al. Loss of autophagy in the central nervous system causes neurodegeneration in mice. Nature 2006;441:880–4. [PubMed: 16625205]

40. Komatsu M, Waguri S, Ueno T, Iwata J, Murata S, Tanida I, et al. Impairment of starvation-induced and constitutive autophagy in Atg7-deficient mice. J Cell Biol 2005;169:425–34. [PubMed: 15866887]

41. Mailleux AA, Overholtzer M, Schmelzle T, Bouillet P, Strasser A, Brugge JS. BIM regulates apoptosis during mammary ductal morphogenesis, and its absence reveals alternative cell death mechanisms. Dev Cell 2007;12:221–34. [PubMed: 17276340]

42. Pearson JF, Hughes S, Chambers K, Lang SH. Polarized fluid movement and not cell death, creates luminal spaces in adult prostate epithelium. Cell Death Differ 2009;16:475–82. [PubMed: 19096393]

43. Kang C, You YJ, Avery L. Dual roles of autophagy in the survival of Caenorhabditis elegans during starvation. Genes Dev 2007;21:2161–71. [PubMed: 17785524]

44. Shimizu S, Kanaseki T, Mizushima N, Mizuta T, Arakawa-Kobayashi S, Thompson CB, et al. Role of Bcl-2 family proteins in a non-apoptotic programmed cell death dependent on autophagy genes. Nat Cell Biol 2004;6:1221–8. [PubMed: 15558033]

45. Pattingre S, Tassa A, Qu X, Garuti R, Liang XH, Mizushima N, et al. Bcl-2 antiapoptotic proteins inhibit Beclin 1-dependent autophagy. Cell 2005;122:927–39. [PubMed: 16179260]

46. Knecht E, Hernandez-Yago J, Grisolia S. Regulation of lysosomal autophagy in transformed and non-transformed mouse fibroblasts under several growth conditions. Exp Cell Res 1984;154:224–32. [PubMed: 6088263]

47. Huang J, Klionsky DJ. Autophagy and human disease. Cell Cycle 2007;6:1837–49. [PubMed: 17671424]

48. Jin S, White E. Role of autophagy in cancer: management of metabolic stress. Autophagy 2007;3:28–31. [PubMed: 16969128]

49. Mathew R, Kongara S, Beaudoin B, Karp CM, Bray K, Degenhardt K, et al. Autophagy suppresses tumor progression by limiting chromosomal instability. Genes Dev 2007;21:1367–81. [PubMed: 17510285]

50. Yue Z, Jin S, Yang C, Levine AJ, Heintz N. Beclin 1, an autophagy gene essential for early embryonic development, is a haploinsufficient tumor suppressor. Proc Natl Acad Sci U S A 2003;100:15077–82. [PubMed: 14657337]

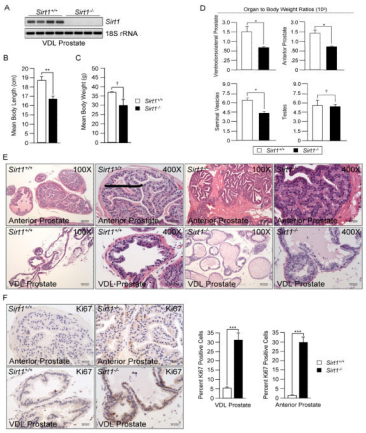

**Figure 1. *Sirt1* Deletion Alters Androgen-Responsive Tissue Development**

(A) RT-PCR using ventrodorsolateral prostate RNA from *Sirt1*$^{+/+}$ and *Sirt1*$^{-/-}$ mice. (B) Mean body length, (C) mass, and (D) select tissue weights normalized to total mass (see also Fig. S1A). (E) Hematoxylin and Eosin (H&E) staining of prostate glands from *Sirt1*$^{+/+}$and *Sirt1*$^{-/-}$ mice (see also Fid. S1B). (F) Ki67 staining of *Sirt1*$^{+/+}$ and *Sirt1*$^{-/-}$ prostates. All data are mean ± standard error of the mean (SEM) and represent n=5/genotype. P values were determined by student's t-test (**P*<0.05, ***P*<0.01, ****P*<0.001, † denotes no statistical significance).

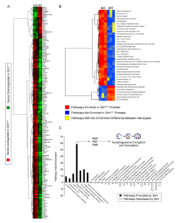

**Figure 2. *Sirt1* Governs Vital Biological Pathways in the Prostate**

(A) Treeview of microarray data generated from *Sirt1*$^{+/+}$ and *Sirt1*$^{-/-}$ ventrodorsolateral prostates. (B) Heatmap displaying pathways affected by *Sirt1* in the prostate as determined by the Analysis of Sample Set Enrichment Scores (ASSESS) database (see also Fig. S1C, Tables S1-S4). (C) Graphical schematic highlighting *Sirt1* affected pathways in the prostate as revealed by the Database for Annotation, Visualization and Integrated Discovery (DAVID). Also illustrated is *Sirt1's* ability to affect a subset of autophagy related genes (*Atg's*) involved in autophagosome maturation and completion.

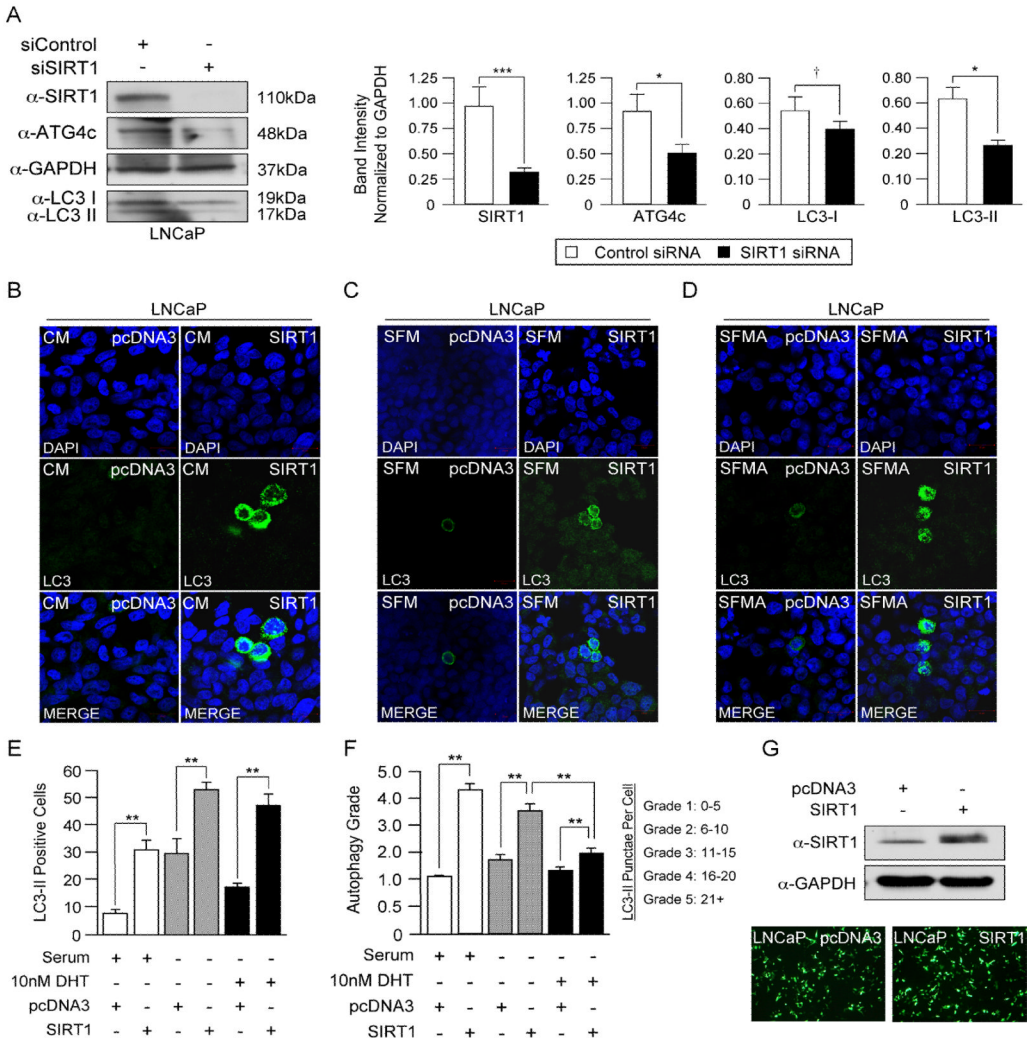


**Figure 3. SIRT1 Antagonizes AR-Mediated Inhibition of Autophagy**

(A) Western blot for SIRT1, ATG4c, and LC3 following SIRT1 siRNA treatment in LNCaP cells. All data are representative of triplicate experiments. Statistical significance was determined by Student's t-test (**P*<0.05, ****P*<0.001, † denotes no statistical significance). (B-D) LNCaP cells transfected with pcDNA3 or SIRT1 and cultured in complete serum media (CM), serum free media (SFM), or serum free media supplemented with 10nM DHT (SFMA) were subjected to LC3-II immunofluorescence (see also Figs. S2A-S2C). (E,F) Quantitation of autophagic cells based on LC3-II positivity (ANOVA, ***P*<0.01) and autophagic grade (Mann Whitney U, ***P*<0.01). All data are representative of triplicate experiments. Quantitation represents at least 100 cells counted and scored per treatment. (G) SIRT1 Western blot following co-transfection with pcDNA3 vector control or SIRT1 and GFP (micrographs confirm GFP-positive cells post-transfection).

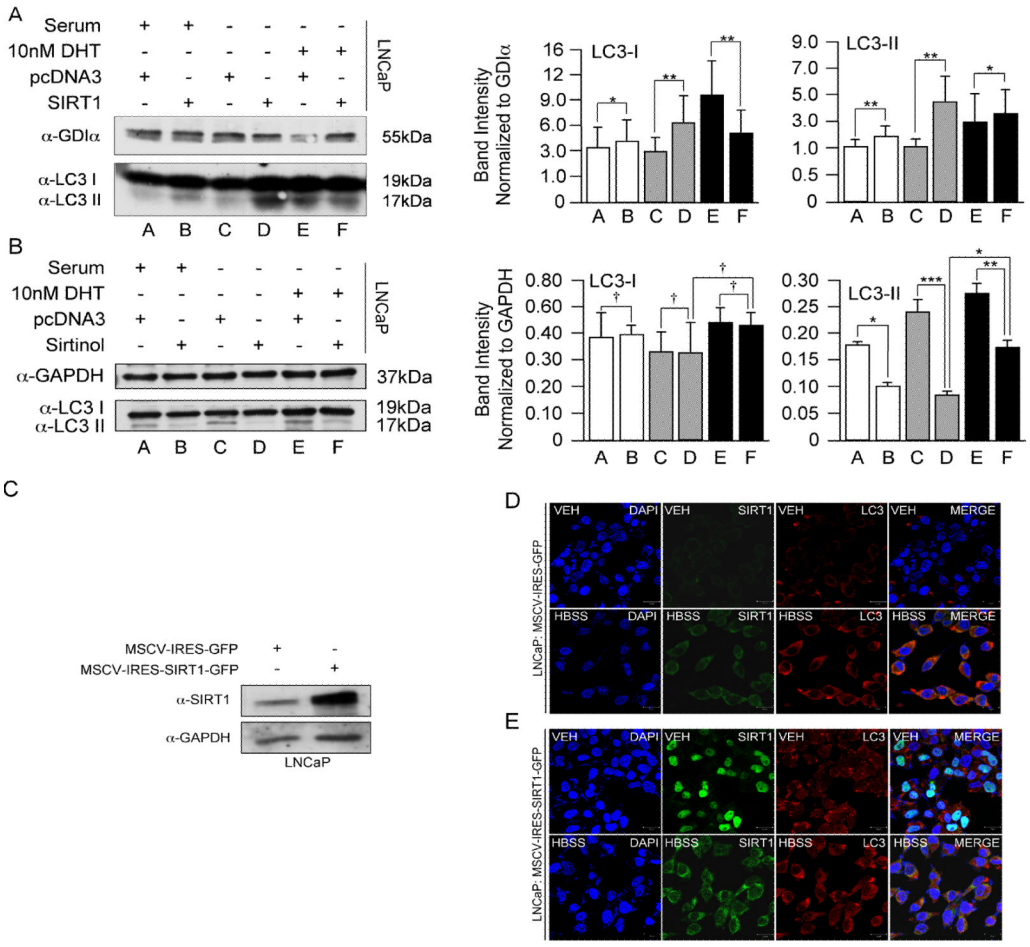


**Figure 4. SIRT1 Promotes Autophagy in Prostate Cancer Cells**

(A,B) LC3 Western blots in LNCaP cells following SIRT1 over-expression or inhibition via Sirtinol (30μM) in various media conditions. (C) Western blot verifying SIRT1 abundance in LNCaP cells transduced with MSCV-IRES-GFP or MSCV-IRES-SIRT1-GFP retroviruses. (D,E) SIRT1 and LC3 dual-immunofluorescence of transduced LNCaPs in the presence or absence of autophagic stimuli (HBSS) (see also Fig. S7). All data are representative of triplicate experiments. Statistical significance was measured by ANOVA (**P*<0.05, ***P*<0.01, ****P*<0.0001, † denotes no statistical significance).

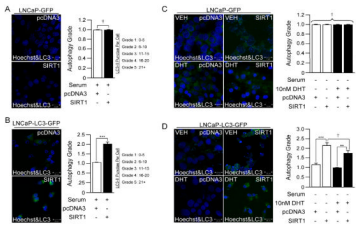

**Figure 5. SIRT1 Enhances LC3 Cleavage and Autophagy Regardless of Media Conditions**

(A,B) LNCaP cells stably expressing GFP (LNCaP-GFP) or a GFP-tagged, pre-cleaved version of LC3 (LNCaP-LC3-GFP) transfected with SIRT1 or pcDNA3 vector control. (C,D) LNCaP-GFP and LNCaP-LC3-GFP cells transfected with pcDNA3 or SIRT1 in the presence and absence of DHT. Quantitation of triplicate experiments was performed based on autophagic grade and graphed adjacent to micrographs (Mann Whitney U, ***P*<0.01, ****P*<0.001, † denotes no statistical significance).

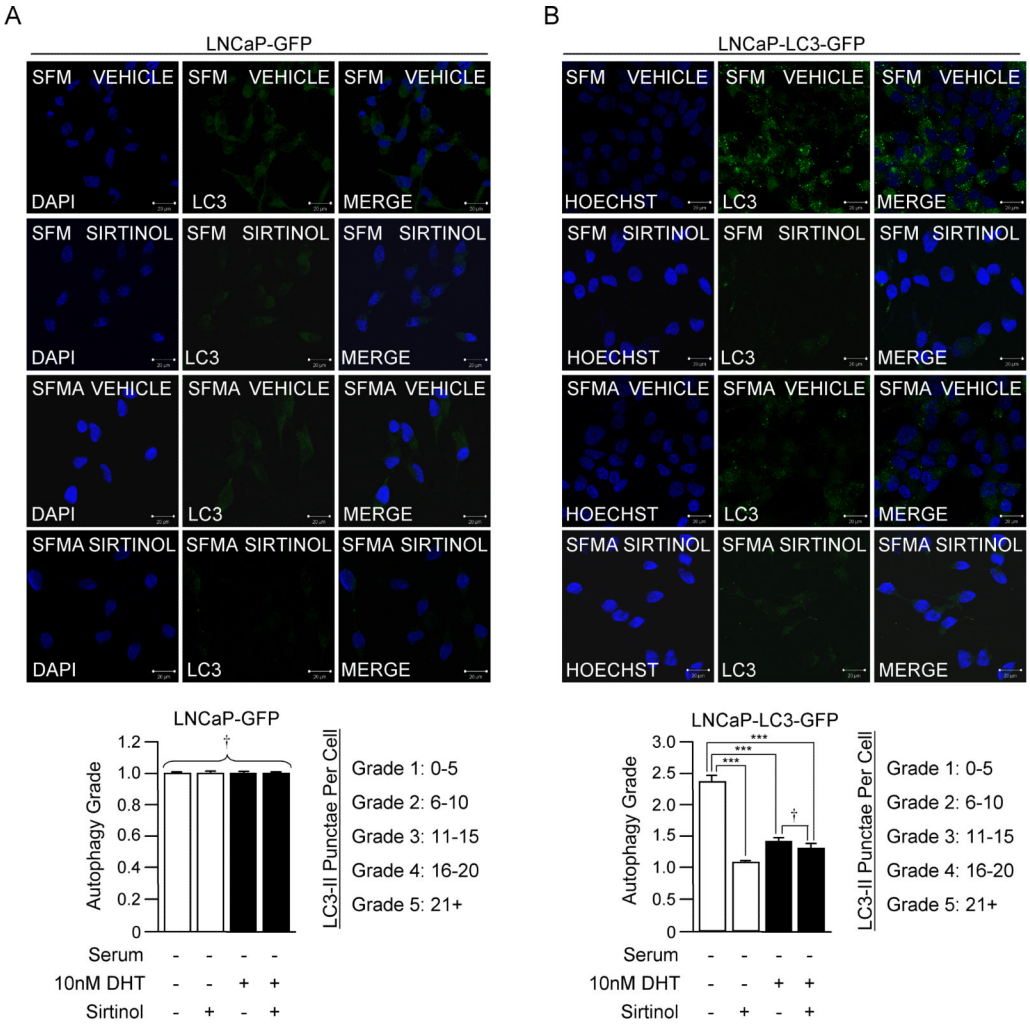


**Figure 6. Chemical Inhibition of SIRT1 Abolishes Autophagy in Prostate Cancer Cells**

(A,B) LNCaP-GFP and LNCaP-LC3-GFP cells cultured in various media conditions in the presence and absence of Sirtinol (30μM) and analyzed by confocal microscopy for LC3 punctae. Statistical significance of triplicate experiments was measured by Mann Whitney U test (***$P$<0.001, † denotes no statistical significance).

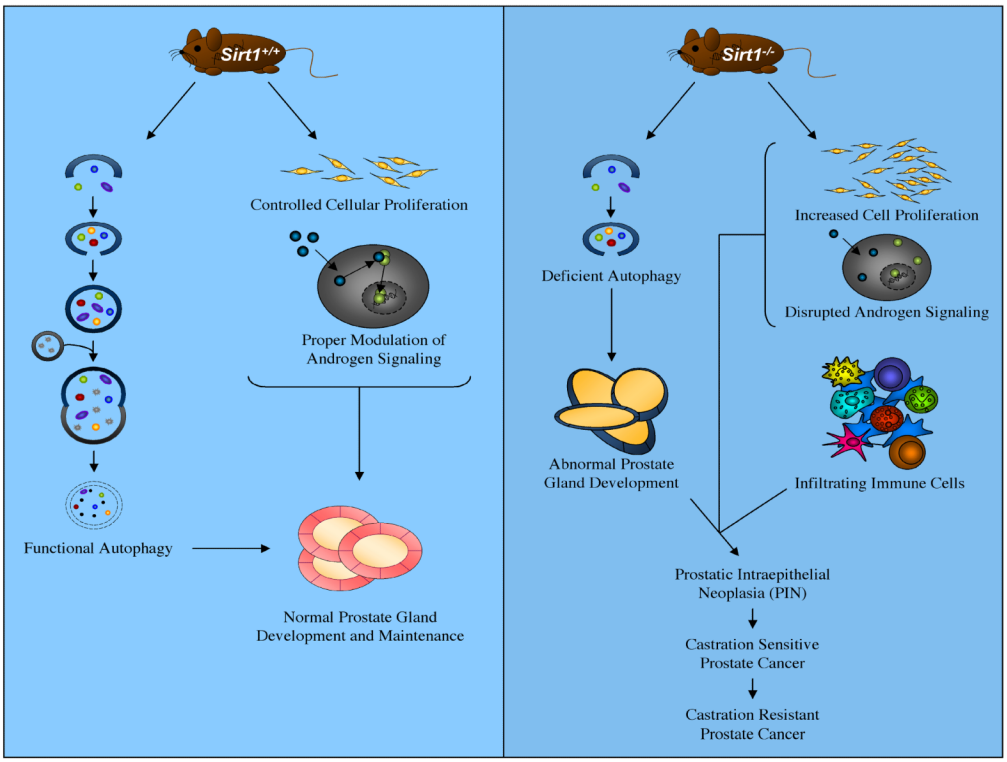


**Figure 7. SIRT1 Promotes Autophagy-Mediated Prostate Development and Health**

(A) Proposed model of SIRT1 function in the prostate as it relates to autophagy and prostate homeostasis.